# DETECTION OF BUILDING DAMAGES DUE TO THE 2001 GUJARAT, INDIA EARTHQUAKE USING SATELLITE REMOTE SENSING

Y. Yusuf[1], M. Matsuoka[2] and F. Yamazaki[3]

## ABSTRACT

In this paper, we present a method of earthquake damage detection, in which optical images with multi-spectral bands are compared, for the Gujarat, India earthquake, which occurred on January 26, 2001. We investigated the pre- and post-earthquake satellite images by calculating the differences in the reflection intensities (digital numbers) of the two images. The estimated damaged area was abstracted on a pixel unit based on the obtained frequency distributions of the differences in the optical sensor values, which showed significant changes in the reflectance due to the earthquake disaster. We investigated the accuracy of our analytical results using a classification method for estimating damaged area based on training data with aerial photographs taken after the earthquake and the damage distribution estimated from SAR images. The damaged areas estimated by all methods are very similar. By presenting a successful method for damage detection using optical images, we confirmed that satellite remote sensing is a very powerful tool for detecting earthquake damage over a large area.

## Introduction

After a large-scale earthquake, satellite remote sensing can be a very useful method of determining damage distribution since remote sensing images cover large areas. Remote sensing data have been used successfully for damage assessment after the 1995 Kobe, Japan and the 1999 Kocaeli, Turkey earthquakes (Matsuoka and Yamazaki 1998; Estrada et al. 2000). Recently, the US military meteorological satellite DMSP, imaging nighttime lights of cities, has been used to estimate the damaged areas (Hayashi et al. 2000).

In this study, we present a method of earthquake damage detection in which the pre- and post-earthquake optical images with multi-spectral bands are compared. The data used in this study is obtained from Landsat-7 satellite images taken before and after the 2001 Gujarat, India earthquake that occurred on January 26. The pre-event image was acquired on January 8, 2001 and the post-event image on February 9, 2001. We compared the spectral responses of the pre- and post-event satellite images by calculating the differences in the digital numbers of the two

[1] Earthquake Disaster Mitigation Research Center, NIED, Miki City, Hyogo, Japan 673-0433
[2] Deputy Team Leader, Earthquake Disaster Mitigation Research Center, NIED, Miki City, Hyogo, Japan 673-0433
[3] Team Leader, Earthquake Disaster Mitigation Research Center, NIED, Miki City, Hyogo, Japan 673-0433

images in the sample area. The estimated damaged area was abstracted on a pixel unit based on the obtained frequency distributions of the differences in the optical sensor values, which showed significant increase in reflectance due to the earthquake disaster. The accuracy of our analytical results was investigated, comparing with aerial photographs (IITB & EDM 2001). The damaged area was also estimated using RADERSAT SAR images.

## Satellite Images and Study Area

Landsat-7 was launched on April 15, 1999. The altitude of Landsat-7 is approximately 705 km with a recurrence period of 16 days. The earth-observing instrument on Landsat-7, the Enhanced Thematic Mapper Plus (ETM+), replicates the capabilities of the highly successful Thematic Mapper (TM) instruments on Landsat-4 and 5. ETM+ is an advanced, multi-spectral scanning, earth resources sensor designed to achieve higher image resolution, sharper spectral separation, more improved geometric fidelity and greater radiometric accuracy and resolution than those of TM. ETM+ data are obtained in eight spectral bands simultaneously. Band 6 corresponds to thermal (heat) infrared radiation. ETM+ scene has a spatial resolution of 30 meters for bands 1-5 and 7 while band 6 has a 60-meter spatial resolution and the panchromatic band has a 15-meter spatial resolution (NASDA 2001).

Figure 1 shows typical reflectance curves for three basic types of earth features: green vegetation, dry bare soil and water. The lines in this figure represent the average reflectance curves compiled by measuring a large sample of features, which reveal some fundamental points concerning spectral reflectance. Since band 6 has a low spatial resolution, only the multi-spectral bands 1-5 and 7 are used in this study.

Figure 2 shows the Landsat-7 band 1 satellite image before the Gujarat earthquake. The Anjar and Banni Plain regions were selected as the target areas (Figure 2). In the image, effects of cloud cover are found to be minimal. Image registration was carried out as a preprocessing procedure.

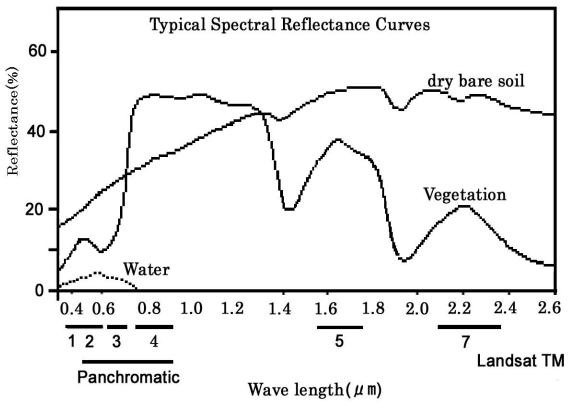


Figure 1. Typical reflectance curves for vegetation, soil and water.

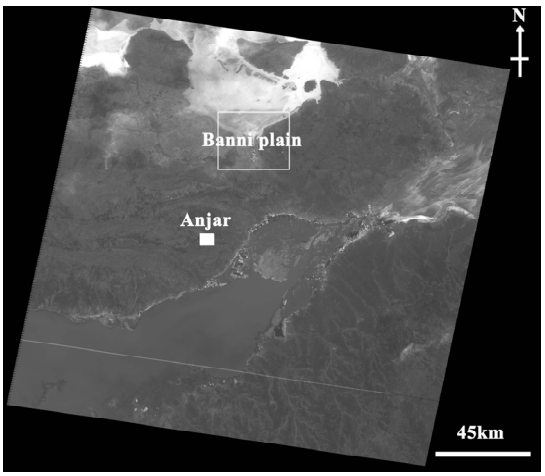


Figure 2. Landsat-7 band 1 image before the earthquake.

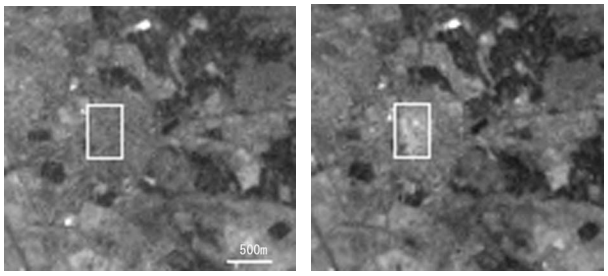


(a) Pre-earthquake (b) Post-earthquake

Figure 3. Landsat-7 images of Anjar (Band 1).

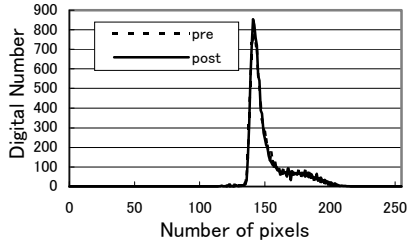


Figure 4. Histograms of NDVI value for the pre- and post-earthquake images.

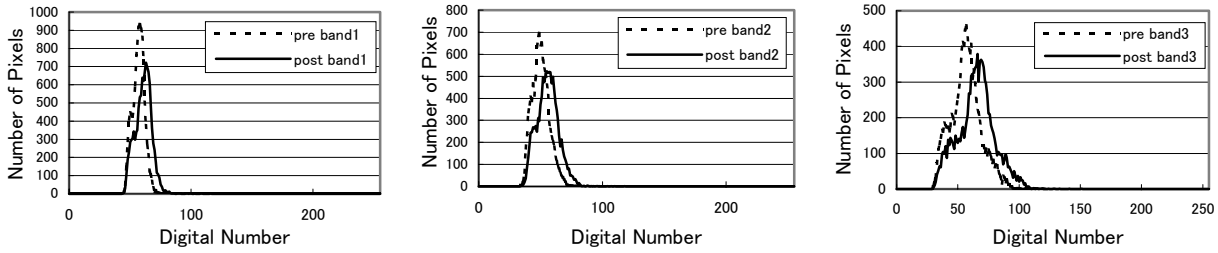


(a) Band 1 (b) Band 2 (c) Band 3

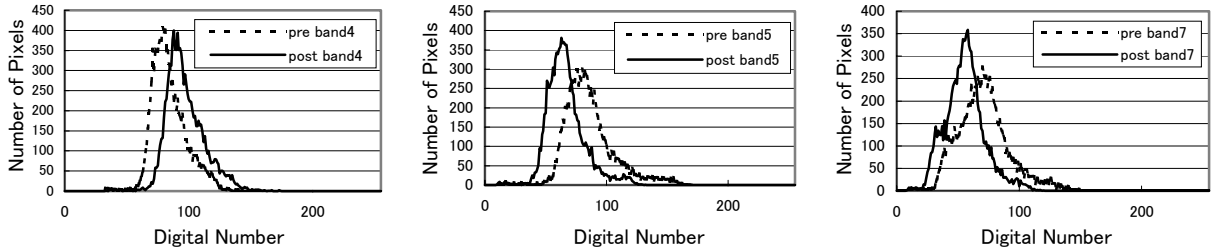


(d) Band 4 (e) Band 5 (f) Band 7

Figure 5. Histograms for the pre- and post-earthquake images of Anjar.

Figure 3 shows the target area abstracted from the pre- and post-earthquake images of band 1. The pixel value in the post-earthquake image is found to be much higher than that in the pre-earthquake image. To evaluate the influence of the season, the normalized difference vegetation index (NDVI) was calculated using the following equation for each of the pre- and post-earthquake images.

$$NDVI = (NIR - R)/(NIR + R) \times 127 + 127 \qquad (1)$$
$$(0 \leq \text{NDVI} < 255)$$

Here, band 4 was used for the NIR (near-infrared) and band 3 was used for the R (visible infrared). Theoretically, the NIR is scattered by the vegetation, and the R is absorbed by chlorophyll. Hence NDVI becomes large when there is abundant vegetation covering the surface of the earth. Figure 4 shows the histograms of NDVI of the pre- and post-earthquake images. Since the changes of NDVI for the pre- and post-earthquake images are minimal, the influence of the season can be disregarded.

Figure 5 shows the histogram of the digital numbers of multi-spectral bands for the pre- and post-earthquake images. The pixel value in the post-earthquake images for bands 1-4 is found to be much higher than that in the pre-earthquake images (Figure 5(a)-(d)). However, unlike bands 1-4, the pixel value in the post-earthquake images for bands 5 and 7 is found to be lower than that in the pre-earthquake images (Figure 5(e), (f)).

**Detection of Damaged Area**

For the classification of damaged areas we have analyzed the pre- and post-earthquake satellite images by calculating the differences in the digital numbers of the both images. Pixels whose digital numbers have significantly changed are considered to represent the areas of damage due to the earthquake. The damaged area was extracted on a pixel unit based on the obtained frequency distributions of the differences in the optical sensor values, which show significant changes in the reflectance. Figure 6 shows the procedure for determining damaged areas.

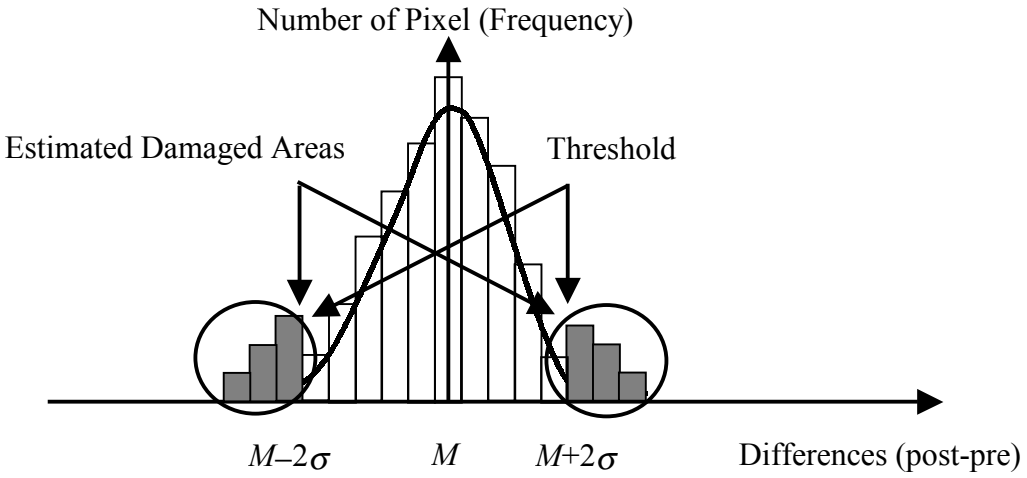


Figure 6. The determination procedure of damaged areas.

The process of damage abstraction is described as follows. First, we calculate the difference in the brightness values of pre- and post-earthquake images. The difference can be represented as a normal distribution. Then we have calculated the mean ($M$) and the standard deviation ($\sigma$) of the difference. If the difference is over $M+2\sigma$, the reflectance of the area is considered to be significantly increased, and if the difference value is less than $M-2\sigma$, the reflectance of the area is considered to be significantly decreased. Both of these areas with significant changes are considered as damaged areas.

Figures 7 and 8 show the analytical results for Anjar and the Banni Plain. The black pixels show the damaged areas. In the case of Anjar, almost all the digital numbers of the pixels of the damaged area extracted from bands 1-4 increased. In the visible to near-infrared images, severe building damage in the urban areas shows higher brightness due to the presence of brick and stone from the collapsed buildings. Good correspondences were shown for most of the damage distributions with the results estimated using the panchromatic band and those identified from the post-earthquake aerial photographs (Yusuf et al. 2001). On the other hand, a few pixels

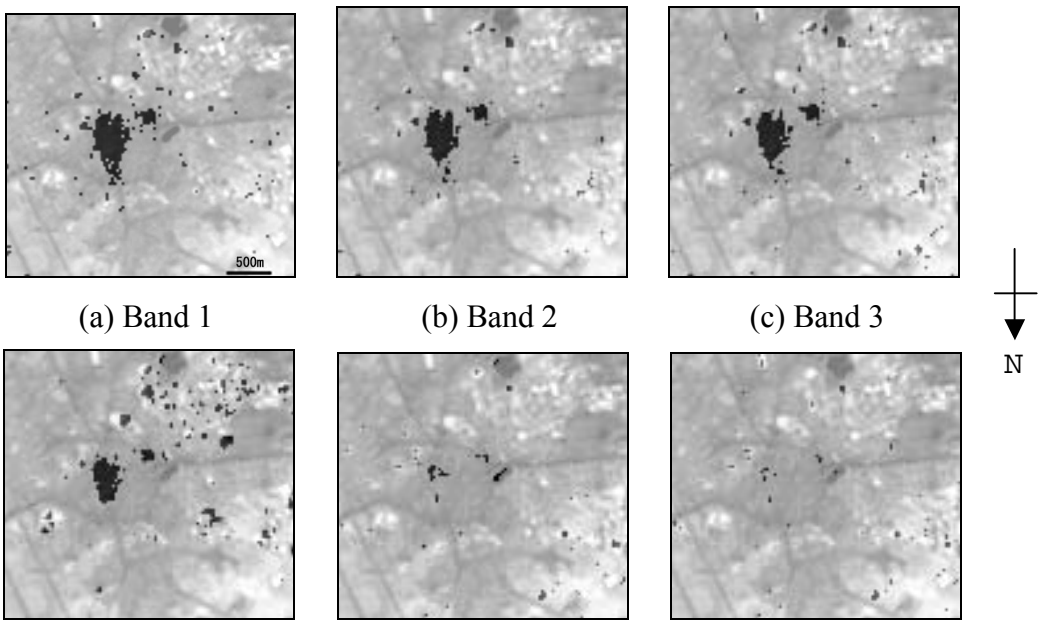


(a) Band 1 (b) Band 2 (c) Band 3

(d) Band 4 (e) Band 5 (f) Band 7

Figure 7. Extracted damaged area of Anjar (black pixels).

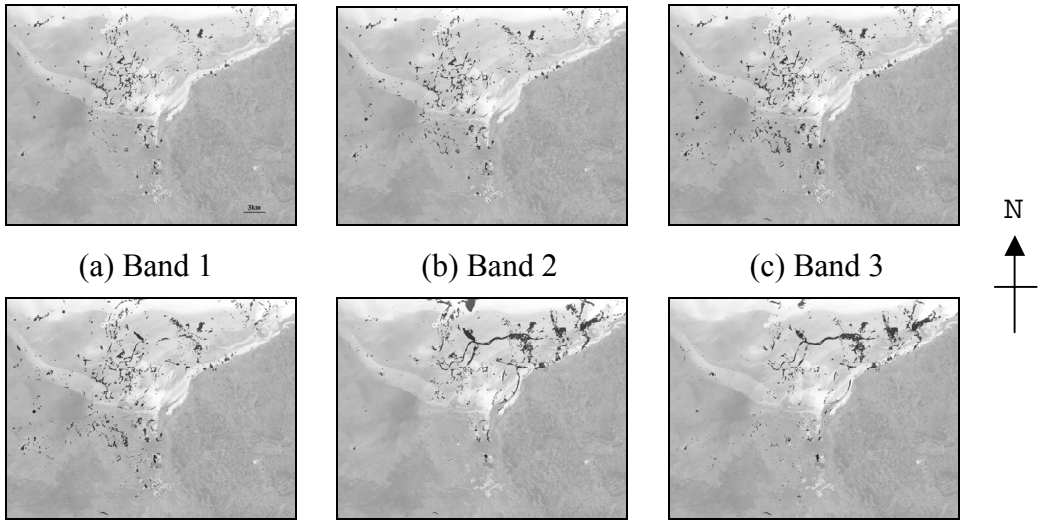


(a) Band 1 (b) Band 2 (c) Band 3

(d) Band 4 (e) Band 5 (f) Band 7

Figure 8. Extracted damaged area of Banni Plain (black pixels).

of damaged areas were extracted from bands 5 and 7 (Figure 9(a)). To investigate the reason for this, we calculated the ratio of band 5 to 7 (Band7/Band5) for the pre- and post-images, respectively. As a result, it was found that the histogram of the ratio for the post-earthquake image was in good agreement with that of the pre-earthquake image. The mean of the difference was almost zero and the standard deviation was very small. That is to say, in the pre- and post-earthquake images of the object area, the change of the digital number of band 7 with respect to that of band 5 are very small. The possibility that the significant difference (Figures 5 (e), (f)) observed between the histograms of bands 5 and 7 for the pre- and post-earthquake images is due

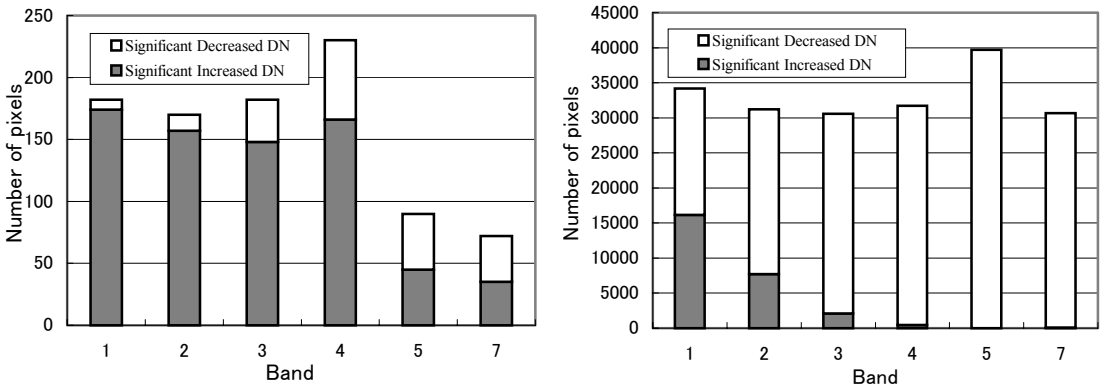


(a) Anjar (b) Banni Plain

Figure 9. Extracted number of damaged pixels.

to of the difference in the observation environment, such as sunlight and the atmosphere.

Figure 9 (b) shows the number of pixels extracted as damaged areas in the Banni Plain. Numerous pixels with reduced brightness were extracted from bands 5 and 7 around this region. In this area, during the rainy season, the ground is saturated with water, and during the dry season, the water table drops and the salt in the water spreads on the surface of the earth. Both before and after the earthquake, this area is characterized by very high brightness due to the presence of salt. However, after the earthquake, muddy groundwater gushed to the surface due to liquefaction (The University of Memphis 2001; IIT 2001). Since there is almost no reflectance of water in these two bands, it is conceivable that the areas where the brightness value decreased correspond to muddy water. Thus the brightness level of pixels appeared to be lower in the post-earthquake satellite image. On the other hand, because there is a slight reflection by water in bands 1-4, a few pixels of reduced brightness are still extracted. The number of extracted pixels decreases with shorter observation wavelength.

## Evaluation of the Results of Extracted Damaged Areas

To investigate the accuracy of the results of extracted damaged areas, we first present a simple classification method for estimating the damaged area using training data that was selected based on an aerial photograph (Figure 10) taken 16 days after the earthquake. We also compared with the results of estimated damaged areas obtained using SAR images. Anjar was selected as the target area for both comparisons. Since bands 5 and 7 were not suitable for abstracting urban damaged areas as we described above, only bands 1-4 were used for the classification of optical images.

### Estimated Damaged Areas Using Training Data

Many methods of classification using digital images of training data exist, such as the maximum likelihood classifier and the minimum-distance-to-mean classifier. To realize high accuracy using these classification methods, numerous sample elements and ground-truth data are required. In this study, we apply a simple classification method. We assume that the pixel values have a normal distribution. First, the training data are created from the original image for

a training area. Then, the classification is preformed using equation (1):

$$M - 2\sigma \le P \le M + 2\sigma \qquad (1)$$

where $M$ and $\sigma$ are the mean and the standard deviation of the extracted training data, respectively, and $P$ is the digital number of a pixel to be classified. If the pixel value satisfies equation (1), then this pixel is classified into the same class. Based on this classification method, damage extraction for urban areas follows the following four basic steps.

Figure 10. Aerial photograph taken after the earthquake.

(1) Preparation of Training Data

The rectangular area in Figure 3 is selected as the training area, where the brighter areas appearing in the post-earthquake image represent locations of severe damage, as identified by the aerial photographs.

(2) Abstraction of Urban Areas

The mean and standard deviation of pixel values of the training area are calculated using the pre-earthquake image. The pixels belong to urban area are classified using equation (1).

(3) Abstraction of Damaged Areas

For the extraction of damaged areas, instead of using a pre-earthquake image, only a post-earthquake image is used.

(4) Abstraction of Damaged Urban Areas

Damaged urban areas are extracted by integrating the images obtained in steps (2) and (3) (Figure 11).

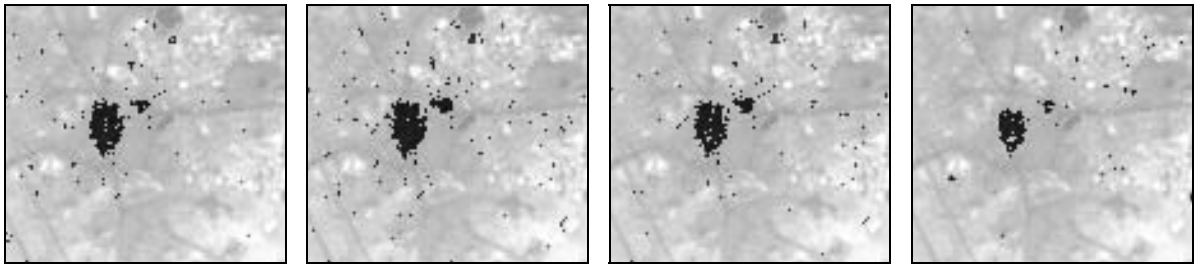

(a) Band 1 (b) Band 2 (c) Band 3 (d) Band 4

Figure 11. Extracted damaged area of Anjar based on the training data (black pixels).

## Estimated Damaged Areas from SAR Images

One of the remarkable characteristics of synthetic aperture radar (SAR) is the capability to record a physical value, called the backscattering coefficient, of the earth's surface independent of weather and sunlight conditions. Therefore SAR may possibly be used to develop a universal method for identifying damaged areas due to natural disasters such as earthquakes, forest fires and floods. After our feasibility study on the backscattering characteristics of areas damaged by the 1995 Kobe earthquake using the pre- and post-event ERS images, the backscattering coefficient and the intensity correlation for post-event ERS images were found to become low in hard-hit areas, as shown in Figure 12 (Aoki et al. 1998). Then, we obtained an optimum window size for evaluating building damage using the above indices derived from the pre- and post-event images and proposed an unsupervised method for estimating areas of severe building damage (Matsuoka and Yamazaki 2001).

SAR images were taken over Anjar city on December 12, 1999 and February 11, 2001 by the Canadian satellite, RADARSAT, whose spatial resolution is approximately 9 meters, because of its fine mode acquisition. The damage detection method developed for the dataset of the Kobe earthquake was applied to this Indian event. The estimated damage distribution is shown in Figure 13 (black color).

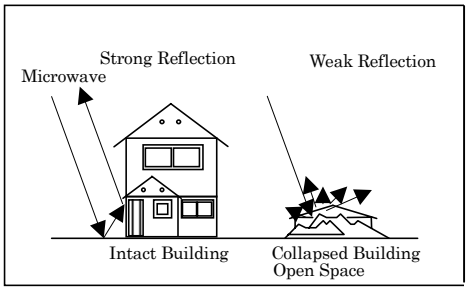


Figure 12. Schematic diagram of backscattering characteristics of built-up areas.

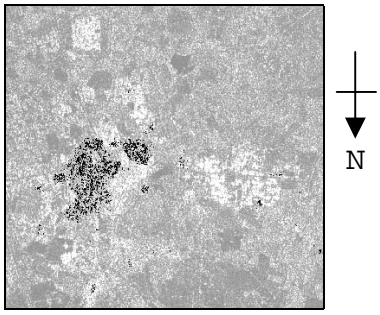


Figure 13. Estimated building areas (black) in Anjar using pre- and post-damage event RADARSAT SAR images.

The results estimated using the method presented in this paper are relatively in good agreement with the results obtained using the training data based on the aerial photographs and SAR images. Therefore we can conclude that the method presented in this paper is adequate for estimating the damaged area using optical images.

## Conclusions

For the purpose of identifying earthquake damage at an early stage after a large-scale earthquake using satellite images, we presented a method of damage detection in which the optical images with multi-spectral bands taken by the Landsat-7 satellite are compared. The damaged areas from the 2001 Gujarat, India earthquake were extracted by calculating the difference in the digital numbers of the post- and pre-earthquake images. Good correspondences were shown for most of the damaged distributions that resemble the estimated results using the classification method with training data, and the damaged areas identified from the post-

earthquake aerial photographs. For the multi-spectral bands of Landsat-7, the use of bands 1-4 is effective for the extraction of city damage area and the use of bands 5 and 7 is effective for the extraction of changes from the areas of water coverage or the areas of liquefaction.

Due to the lack of detailed damage survey data, the accuracy of these analytical results still need further verification. In the future, we will discuss the relationship between the damage level and the value of digital numbers, based on detailed damage survey data.

## Acknowledgments

The Landsat and RADARSAT images used in this study are owned by the U. S. Government and United Sates Geological Survey (USGS), and Canadian Space Agency (CSA), respectively.

## References

Aoki, H., M. Matsuoka, and F. Yamazaki (1998). Characteristics of Satellite SAR Images in the Damaged Areas due to the Hyogoken-Nanbu Earthquake, *Proceedings of the 19th Asian Conference on Remote Sensing*, C7, 1-6.

Estrada, M., M. Matsuoka, and F. Yamazaki (2000). Use of Optical Satellite Images for the Recognition of Areas Damaged by Earthquakes, *6th International Conference on Seismic Zonation*, 103-108.

Hayashi, H., S. Hashitera, M. Kohiyama, M. Matsuoka, N. Maki, H. Fujita, and C. D. Elvidge (2000). International Collaboration for the Early Damaged Area Estimation System Using DMSP/OLS Nighttime Images, *Proceedings of IEEE 2000 International Geoscience and Remote Sensing Symposium* (CD-ROM).

India Institute of Technology Bombay (IITB), India, and Earthquake Disaster Mitigation Research Center (EDM), Japan (2001). *The Bhuj Earthquake of January 26*.

India Institute of Technology (IIT) (2001). *http://home.iitk.ac.in/^ramesh/gujarat/gujarat.htm*.

Matsuoka, M., and F. Yamazaki (1998). Identification of Damaged Areas due to the 1995 Hyogoken-Nanbu Earthquake using Satellite Optical Images, *Proceedings of the 19th Asian Conference on Remote Sensing*, Q9, 1-6.

Matsuoka, M., and F. Yamazaki (2001). Image Processing for Building Damage Detection due to Disasters using SAR Intensity Images, *Proceedings of the 31st Conference of the Remote Sensing Society of Japan* (in Japanese, in press).

NASDA (2001). *http://landsat.gsfc.nasda.gov/main/documentation.html.*

The University of Memphis (2001). *http://www.ceri.memphis.edu/gujarat/report/sld008.htm*.

Yusuf, Y., M. Matsuoka, and F. Yamazaki (2001). Damage Detection from Landsat-7 Satellite Images for the 2001 Gujarat, India Earthquake, *Proceedings of the 22nd Asian Conference on Remote Sensing* (in press).